International Journal of Shape Modeling, Vol. 8, No. 2 (December 2002) 139–158

SHAPE-COVERING FOR SKELETON EXTRACTION

MICHELA MORTARA, GIUSEPPE PATANÈ
Istituto di Matematica Applicata e Tecnologie Informatiche
Consiglio Nazionale delle Ricerche
Via De Marini 6, 16149 Genova, Italia
e-mail: {michela,patane}@ima.ge.cnr.it

This paper deals with the definition of abstraction tools for deriving high-level descriptions of complex shape models. Among the wide range of shape descriptors, topological graph-like representations provide a powerful and synthetic sketch of the object, and also capture its inner structure, that is how features connect together to give the overall shape. This aspect makes them useful to describe complex 3D objects in various applications as modelling, morphing, matching and recognition. The approach therein presented deals with the extraction of protrusion-like features of the input object based on a multi-scale curvature evaluation of its surface; then, a skeleton is constructed by taking the tips of the protrusions as seed points for expanding topological rings on it.

Keywords: shape understanding, Reeb graph, skeleton, curvature.

1. Introduction

A possible approach to the problem of shape classification and understanding is to represent shape properties of a given object through shape descriptors which are useful to detect those characteristics which are invariant to position, orientation and local noise. Among all, descriptors based on geometry and topology are suitable for dealing with the definition of basic models for representing and generating shapes. For these reasons, an increasing attention has been focusing on the formalization of shape as a combination of geometry, topology and semantics in order to define tools for assessing the similarity among different models. Shape interpretation is especially relevant for the perception of complex forms, where the ability of varying the level of descriptive abstraction is the key for recognizing and classifying highly complex shapes through a multi-resolution framework which abstracts the object at different levels of detail. From a mathematical point of view, classical tools as Morse theory, homotopy and homology appear to be appropriated to deal with topological questions in computer graphics applications [8,9].

The Reeb graph [20, 22] abstracts the input object starting from the study of its critical points with respect to a continuous map; when the height function is chosen, the graph results in an intuitive representation and it is useful for object compression, even thought it does not distinguish between structural and detail features. Furthermore, the description is not affine-invariant depending on the direction of the chosen height function and providing different graphs according to the position of the object in space.

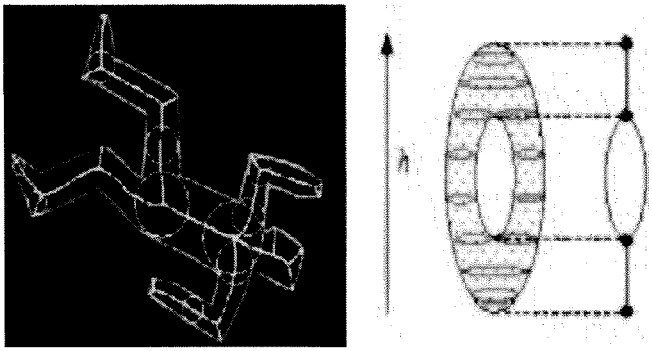

(a) (b)

Fig. 1. (a) Medial Axis Transform, (b) Reeb graph with respect to the height function.

Another skeletal representation for planar shapes is the Medial Axis Transformation, defined by Blum in [3]; the Medial Axis is independent of the object position in space, but it is not stable to small perturbations.

As underlined by Wyvill in [25], a shape description independent of any coordinate system and able to distinguish between meaningful features and details is still lacking. All previous methods for shape abstraction are based on geometric and topological information, e.g. curvature and geodesics, on the input surface. Following previous considerations, we present an affine-invariant skeletal representation of triangle meshes [17] starting from high-curvature regions of the input surface, extracted using the method detailed in [18]. We also prove that this skeleton is a Reeb graph with respect to the topological distance from global features defined by curvature extrema [7, 18].

The paper is organized as follows: the curvature estimation on triangle meshes is briefly described in Section 2. The mathematical definition of the graph as a quotient space is given in Section 4, while its properties and a comparison with the Reeb graph is provided in Section 5. Future work and results are presented in the last section.

1.1. *Review of related work*

The aim of skeleton extraction is to take out and convert shape characteristics and properties of the surface into a compact representation. One of the best known shape descriptors is the Medial Axis Transformation, defined by Blum in [3] for 2D shapes and extended to 3D data sets by Sherbrooke [21]. In the planar case, the Medial axis of a shape is a graph defined as the locus of the centers of all the maximal discs contained inside the surface and having at least two points of contact with its boundary (see Figure 1(a)). This kind of representation is independent of the object position in space (invariance), but tiny perturbations of the boundary produce extra edges in the graph, with no distinction between main and secondary features.

Another method which is used for shape description, and strictly related to our method, is the Reeb graph [1, 2, 20] whose definition is based on Morse theory [15, 22]. First of all, Morse theory states that the topology of a given manifold M can be studied by analyzing the critical points of any smooth function $h : M \mapsto \mathbf{R}$ defined on M. Typically, the map h represents the height function ($\forall p = (x, y, z) \in \mathbf{R^3}$, $\mathbf{h(x, y, z) = z}$) whose critical points, i.e. peaks, pits and passes, are useful for

shape description because they locate regions where morphological changes occur.

Starting from Morse theory, the Reeb graph [20] is defined by coding the evolution of the level sets on M with respect to h, $M_a := \{x \in M : h(x) = a\}$, $\forall x \in \mathbf{R}$, as described by the following definition (see Figure 1(b)).

Definition 1 *Let $h : M \mapsto \mathbf{R}$ be a real valued function on a compact manifold M. The* Reeb graph of M with respect to *h is the quotient space of $M \times \mathbf{R}$ defined by the equivalence relation $\sim$, given by $(p, h(p)) \sim (q, h(q))$, $p, q \in M$, if and only if*

- *$h(p) = h(q)$,*
- *p, q are in the same connected component of $h^{-1}(h(p))$.*

Indeed, the Reeb graph is a 1-dimensional skeleton provided by a continuous scalar function on M and it changes choosing different maps for the definition of $\sim$.

Even if several extensions of this theory [1, 2, 22] have been proposed, the Reeb graph suffers of at least two problems. Firstly, it depends on the chosen map h and, secondly, there is not distinction between large and small features due to the fact that different connected components are collapsed into the same class without distinction of their sizes.

Because the height function is not affine-invariant, in [11] a new map, based on the geodesic distance from a source point $p \in S$, has been defined to overcome this problem. The determination of p is not simple and the solution proposed by the authors is to define, for every point $x \in S$, $h(x)$ as the sum of all geodesic distances $g(x, p)$ from x to p when p varies on the input manifold, that is,

$$h(x) := \int_{p \in S} g(x, p) dp.$$

This function is not invariant to scaling of the object and it is replaced by its normal representation defined as

$$\forall x \in S, \qquad h_n(x) := \frac{h(x) - \min_{x \in S}\{h(x)\}}{\max_{x \in S}\{h(x)\}}.$$

The approach to shape description described in [13, 26] deals with the construction of centerlines from unorganized point sets, and later developed for polyhedral objects in [12] . This graph is essentially a tree whose edges connect the barycenters of the level sets of the function given by the shortest approximated geodesic distance to a source point. The resulting skeletal curve depends on the appropriate choice of the order of the neighborhood graph, on the location of the source point and on the number k of level sets which slice the surface. To choose the seed point an heuristic is used which seems to work well on elongated tubular shapes such as blood vessels and bones; furthermore, examples are given to show that on these kinds of input data the centerlines obtained with different source points are nearly the same. However, the choice of only one seed point determines a privileged slicing direction; this element and a wrong choice of k can lead to the loss of some features if the object is not strictly cylindrical (such as the ear of the horse in Figure 2(a)).

1.2. *Overview of the technique and contributions*

The proposed construction of the skeleton of a 3D object represented by a triangle mesh is made in three steps.

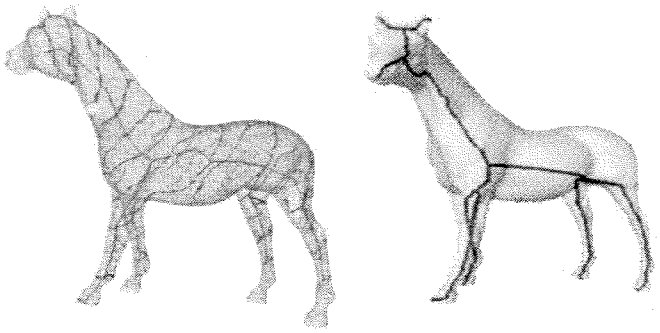

(a) (b)

Fig. 2. (a) Level sets and skeletal curves computed on the horse point set, as shown in [13], (b) result obtained with our algorithm.

1. A curvature estimation is performed on the mesh and several zones of high curvature, which identify the surface features, are extracted (see Figure 3(a)). The procedure of curvature estimation is discussed in Section 2 and it is based on a novel technique detailed in [7, 18]. The idea is to detect points which identify "global" curvature features and to create a hierarchy of such elements with respect to their scale.

2. Starting simultaneously from the centroids of the high curvature regions, topological rings consisting of vertices which have the same topological distance (minimum number of edges) from the nearest centroid are computed, growing of one edge at a time, until the surface is covered (see Figure 3(b)).

3. The centroid of all high curvature regions become the terminal nodes of the graph, while points of split or collision between topological rings during the expansion phase individuate its branching nodes. The centroids of consecutive rings are connected to form an edge (see Figure 3(c)).

2. Curvature estimation on triangular meshes

In this section, the vertex classification into morphological features is briefly discussed focusing on the detection of global protrusions as high-curvature regions only. For more details, we refer the reader to [18].

Let $x : D \subseteq \mathbf{R^2} \mapsto \mathbf{R^3}$ be a C^2-parameterization of the surface

$$\Sigma := \{x(u, v) : (u, v) \in D\}.$$

The classification of local properties of Σ is traditionally based on the study of the *mean* and the *Gaussian* curvature, which can be respectively defined as the average and the product of the maximum and minimum principal curvatures [14].

The Gaussian curvature represents a measurement at any point p of Σ which is the excess per unit area of a small patch of the surface, i.e., how *curved* it is. An interesting result is due to the Gauss-Bonnet theorem, which is introduced as follows. First of all, given a closed curve γ on a surface Σ, let T_γ be the total turning that the unit tangent t undergoes when it is carried along γ, defined as the sum of the local turnings, i.e. *exterior angles* [14] (see Figure 4). Then, the quantity $I_\gamma = 2\pi - T_\gamma$ is called the *angle excess* of the curve γ and it is related to the curvature of Σ within γ, as described by the Gauss-Bonnet formula.

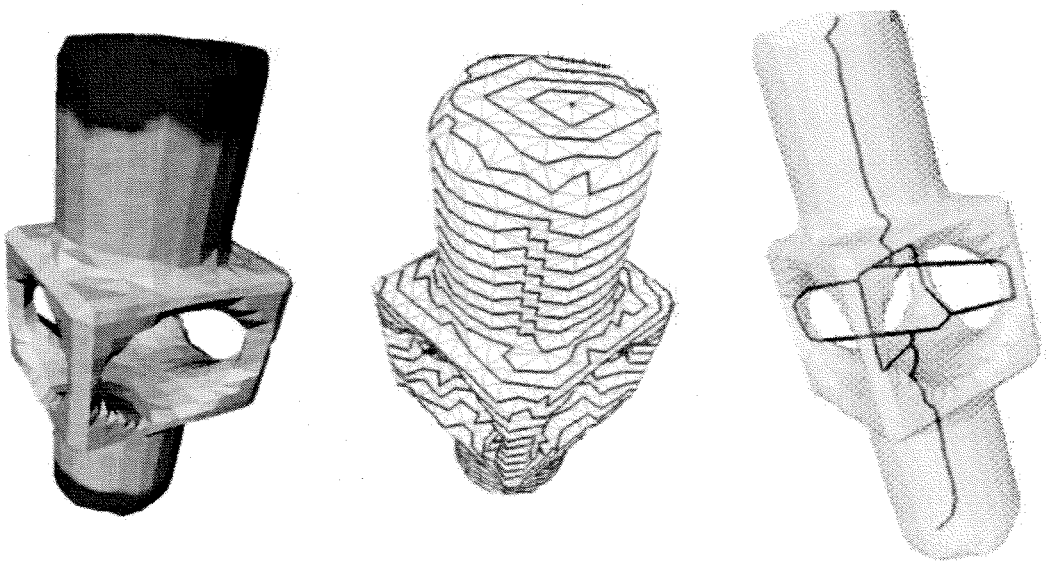

(a) (b) (c)

Fig. 3. Overview of the main steps of the proposed approach: (a) high-curvature regions, (b) topological ring expansion, (c) skeleton.

Gauss-Bonnet Theorem 1 *Let γ be a curvilinear polygon of class C^2 on a surface patch of class C^k, $k \geq 3$. Suppose γ has a positive orientation and its interior on the patch is simply connected. Then*

$$\int_{\gamma} \kappa_g ds + \iint_{\Omega} K dS = 2\pi - \sum_i \alpha_i = I_{\gamma} \tag{1}$$

where κ_g is the geodesic curvature along γ, Ω is the union of γ and its interior, K is the Gaussian curvature, α_i the exterior angles of γ, ds and dS are the curve and line elements respectively.

The definition of the curvature at each point of a triangulation is not trivial because a triangular mesh is parameterized by a piecewise continuous function whose second derivatives are, almost everywhere, null. More precisely, the curvature on a triangulation is concentrated along edges and at vertices, since every other point has a neighborhood homeomorphic to a planar Euclidean domain whose Gaussian curvature is null.

The methods proposed in the literature for curvature evaluation can be divided into two main groups: *continuity-based* and *property-based* algorithms. The first ones are developed transforming the discrete case to the continuous one by using a local fitting of the surface which enables to apply standard definitions. For example, in [10] an approximation is derived at each vertex by applying the continuous definition to a least-square paraboloid fitting its neighboring vertices, while in [23] it is evaluated by estimating its tensor curvature. The second class of algorithms defines equivalent descriptors starting from basic properties of continuous operators but directly applied to the discrete settings. The methods proposed in [4] are based on the Laplace-Beltrami operator, the Gauss map and the Gauss-Bonnet theorem guaranteeing the validity of differential properties such as area minimization and mean curvature flow [9].

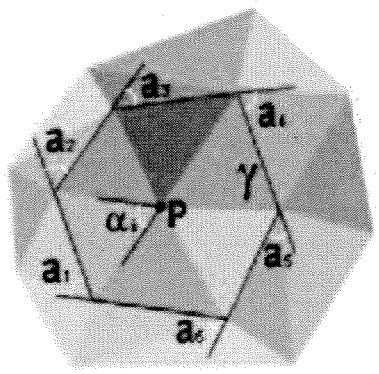

Fig. 4. *Star*(p) is enclosed by a curve γ. The exterior angles $\{a_i\}$ and interior angles $\{\alpha_i\}$ are shown.

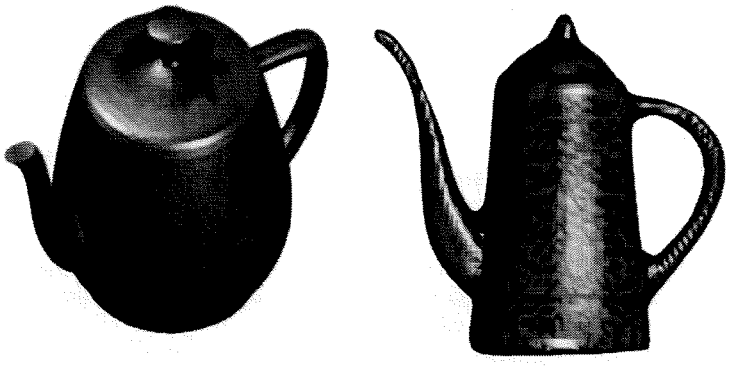

Fig. 5. Gaussian curvature and sensibility to local noise; red and blue vertices represent elliptic and hyperbolic points respectively.

In spite of the introduction of a multi-resolution structure, the mentioned approaches are usually sensitive to noise and small undulations, requiring smoothness conditions on the input mesh. Furthermore, the smoothing process used to get stable and uniform curvature estimations introduces a deficiency in the magnitude evaluation and, consequently, difficulties in the accurate distinction between planar patches and curved surfaces with low curvature. The local dependency to local noise of the curvature estimation is shown in Figure 5.

The angle excess can be used to evaluate the Gaussian curvature at mesh vertices [6, 19]. Let us consider the region *Star*(p) on the surface defined by the triangles incident in a vertex p. The boundary of *Star*(p) defines a closed path on the mesh, to which we may apply the Gauss-Bonnet formula (1). Since the geodesic curvature along the boundary is obviously zero (edges are straight), the total curvature at p is simply quantified by the sum of the exterior angles (see Figure 4).

The approach proposed in [7, 18] for describing a 3D shape integrates boundary and interior information of the shape. The link between closed paths and curvature has suggested to specialize its study to the family of closed paths built by intersecting the surface with spheres centered in each of its points. The study of the evolution of these curves and the geometric characterization of the mesh areas intersected by the spheres are the core of the proposed method.

The topology of the intersection curves changes according to the object shape: in Figure 6(a), the highlighted sphere intersects the surface only at one curve, while in (b) the boundary of the intersection area splits into two connected components. This is likely to happen, for example, near handles and branches, or around deep pits. Therefore, the variation in the boundary suggests that the vertex is in proximity of a feature, which becomes relevant at the scale, or radius, at which the change occurs.

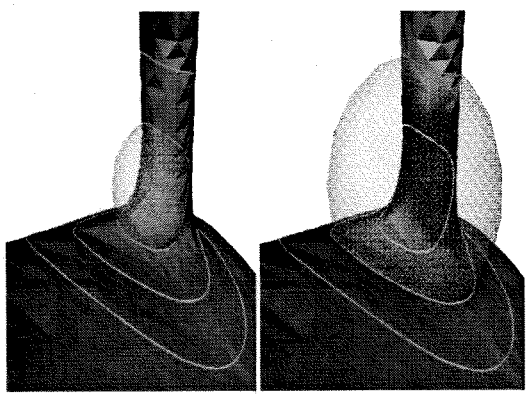

(a) (b)

Fig. 6. The evolution of intersection for increasing radii.

When $\gamma(p, R)$ has only one boundary component, instead of using the angle excess, we evaluate the curvature in p as the length of $\gamma(p, R)$ divided by the radius R, i.e. $L_{\gamma(p,R)} = length(\gamma(p, R))/R$. Note that this value has the dimension of an angle and it always assumes a positive value.

Since we are intended to extract high curvature regions, a threshold is established on the interval $[0, +\infty)$ to locate "sharp" vertices; the less is the value L/R, the more the surface around p tends to a cone shaped surface (see Figure 7)

The method described in [18] proposes a multi-scale vertex classification, that is, curvature evaluation is performed at several scales by using a set of increasing radii each one giving a different decomposition (see Figure 8). It is left to the user to combine, thought a basic query language with boolean operators, features extracted at different scales, or it can be automatically assumed to consider all the protrusions extracted at the different scales. The skeleton construction will start from the selected protrusion set.

3. Graph construction

An object can be seen as made essentially of a main body with several protrusions: for instance, the overall shape of a man consists of the torso from which head, arms and legs depart. From this point of view the main features of a 3D surface are its protrusions, and these are detected by curvature extrema.

Following these considerations, we are going to construct the skeleton of a 3D surface as a graph which, starting from high curvature regions, grows inside the shape towards the main body according to the mutual adjacency among features. First of all, for each high curvature region Γ_i a representative vertex p_i is selected. For a more pleasant visualization p_i is chosen as the centroid of Γ_i and computed as the farthest vertex from the region boundary; anyway, we underline that, from the topological point of view, the arbitrary choice of p_i is irrelevant. Each vertex in the set $\{p_i\}$ represents the terminal node of the graph; we show in the following how

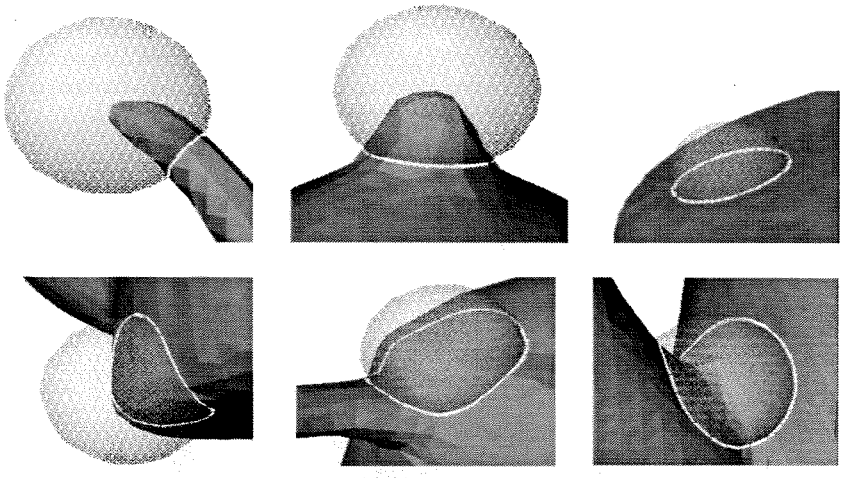

Figure 7: Several cases of one intersection curve: note the relation between the intersection curve length and the curvature of the surface in the neighborhood of the center of the sphere.

the developed algorithm constructs the graph edges and determines the branching nodes according to a topological expansion method. First, some considerations on mesh topology and definitions are given in the following section.

3.1. *Mesh topology*

We represent a triangle mesh S as the pair $S := \{V, F\}$ where $V := \{p_i = (x_i, y_i, z_i) : i = 1, \ldots, N\}$ is a list of N vertices and F is an *abstract simplicial complex* [5] which contains the adjacency information whose subsets come in three types: vertices $\{i\}$, edges $\{i, j\}$ and faces $\{i, j, k\}$. The topology in S is defined by F in the sense that

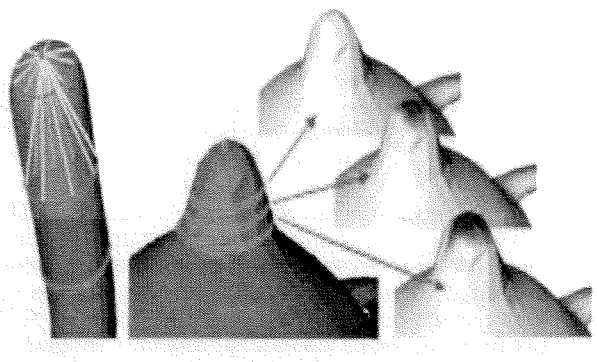

Fig. 8. Curvature evolution with respect to different levels of detail.

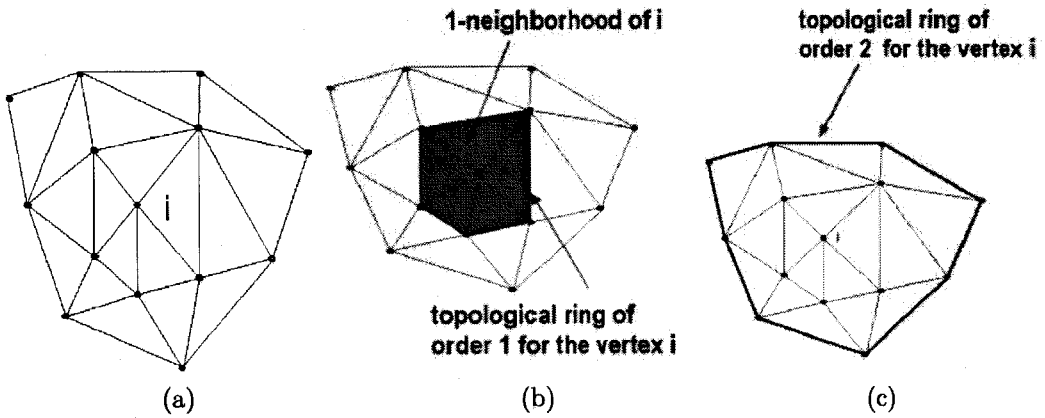

Fig. 9. Local neighborhood system on a triangular mesh: (a) input mesh, (b), (c) topological rings of order 1, 2 for i.

we can construct the *1-neighborhoods* structure as

$$\{N(i) : i = 1, \ldots, N\} \tag{2}$$

with

$$N(i) := \{j \in \{1, \ldots, N\} : (i, j) \in F\}.$$

The previous relation assigns each vertex i the set of its 1-neighborhoods, that is, the vertices j such that (i, j) is an edge of the triangulation F. The size of the neighborhood structure can be recursively enlarged by defining a *n-neighborhood* as

$$\begin{aligned} &N(i_i, \ldots, i_k) := \textstyle\bigcup_{l=1}^{k} N(i_l), \\ &N^0(i) := \{i\}, \\ &N^1(i) := N(i), \\ &N^n(i) := N^1(N^{n-1}(i)),\ n \geq 2. \end{aligned} \tag{3}$$

Indeed, given a vertex $i \in \{1, \ldots, N\}$ we can define its *local neighborhood system* as

$$B_i := \{T(N^k(i)) : k = 0, \ldots\}$$

with

$$T(N^k(i)) := \bigcup_{l,p,q \in N^k(i), \{l,p,q\} \in F} T(l, p, q)$$

and $T(l, p, q)$ triangle with vertices l, p, q. Finally, we refer to the border of $T(N^k(i))$, i.e. $\partial T(N^k(i))$, as *topological ring of order k for i* (see Figure 9).

¿From the previous definitions the following conditions hold: $\forall i \in \{1, \ldots, N\}$

- $v_i \in T(N^k(i)), \qquad k = 0, \ldots$
- $T(N^k(i)) \subseteq T(N^{k+1}(i)), \qquad k = 0, \ldots$
- if S is connected, then

$$S = \bigcup_{k=1,\ldots} T(N^k(i)).$$

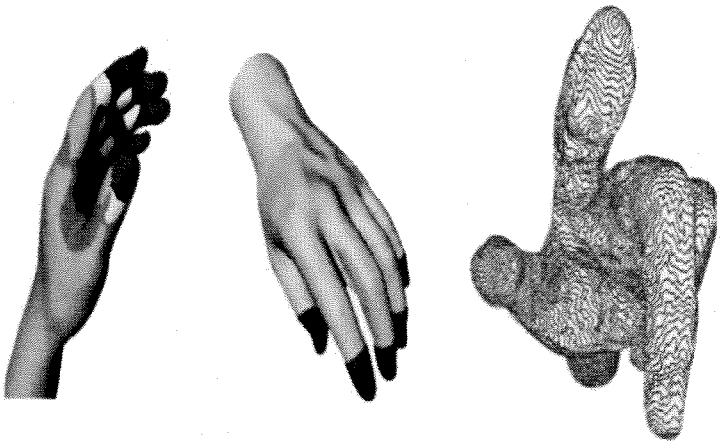

(a) (b) (c)

Fig. 10. (a) Vertex classification on the hand, (b) high curvature regions, (c) topological rings achieved by using the high curvature regions (red areas) as seed points.

3.2. *Topological expansion*

Above this point, we have segmented the mesh into significant/non significant regions, according to the curvature value at each vertex. Because high-curvature regions identify the extremities of the object protrusions, the skeleton of an object characterized in this way has their representative points as terminal nodes. Indeed, for each region a representative vertex is chosen as the farthest, with respect to the topological distance, to the boundary. Starting from the representative vertices we can construct a skeleton of the object using a topological expansion approach, based on the idea of topological rings growing from representative vertices and traversing the mesh, until rings split, collide with others, or can be expanded no more (see Figure 10) .

Starting at the same time from all the representative vertices, the topological rings grow one step at a time until:

- rings belonging to different representative vertices collide: a union occurs,
- a ring intersects itself: a split occurs,
- a ring can be expanded no more: the ring terminates.

Union. When expanding a topological ring we meet a vertex already belonging to the topological ring (of the same order) of another representative vertex, the two rings intersect. From the point of view of the surface, this means that we have found a branching zone of the object where two distinct protrusions depart. In the same way, the corresponding skeleton will have a branch with two edges joining.

The rings of each representative vertices, which determined the collision, can be expanded no more and the construction of their ring sets is completed. A new topological ring is created for the intersection vertex; in this case, unlike what happens for representative vertices, the first topological ring coded is the union of the two rings colliding (see Figure 11(a)).

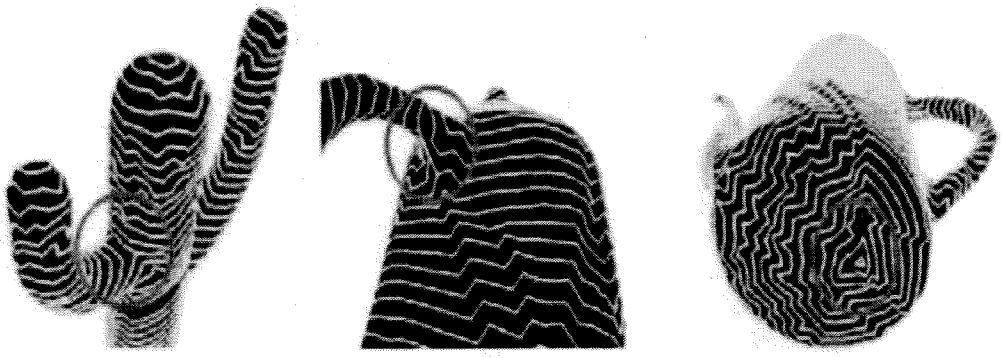

(a) (b) (c)

Fig. 11. Example of (a) union, (b) split, (c) termination.

Split. It can also happen that a ring intersects itself in one or more of its vertices; this is the situation of rings expanding near handles, through holes of the object or where a new protrusion starts. In this case, the intersecting ring splits in two parts and its expansion stops in favor of two new rings derived from the split. Like the union case, the adjacency between the father vertex and the two children is set (see Figure 11(b)).

Termination. After a finite number of steps, the splitting and joining rings will cover the whole surface. A ring terminates when the next step would produce a non valid boundary, that is, with less than three vertices. When a ring terminates, it means that there were no more significant features in the object. Indeed, branches of the skeleton will be not produced in the case of a ring which terminates without having a union or a split (see Figure 11(c)).

3.3. *Graph visualization*

When all the ring sets of the representative vertices and the ones created during their expansion are terminated, the algorithm can draw the skeleton as the adjacency graph encoded during the expansion phase:

- each representative vertex gives a *terminal node*,
- each intersection vertex (occurring in a union or a split configuration) gives a *branching node*,
- the topological rings, belonging to the ring set of a node, give an arc which goes out from that node*. In particular, an arc is drawn by joining the centers of mass of all its topological rings.

In Figure 12 the skeleton of a woman body has been extracted by using high curvature regions located by red areas.

4. Graph as quotient space

*Note that when a split or a union occurs, there can be two arcs going off the same node: in this case two distinct ring sets are created for the same node. So each ring set always defines one node and one arc.

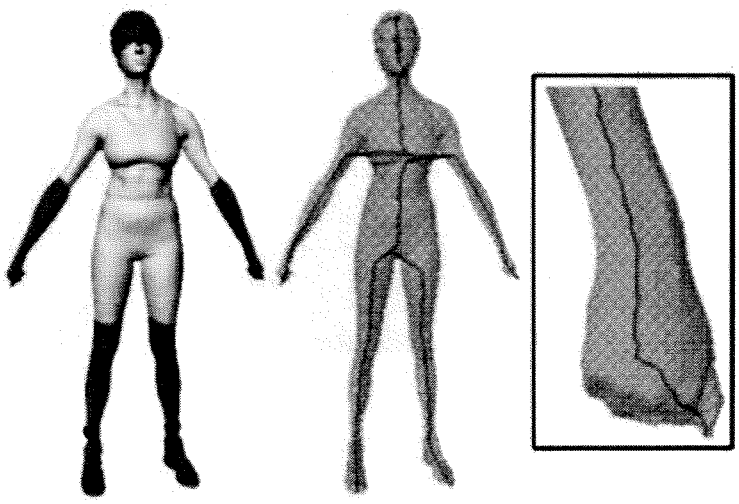

Fig. 12. Example of skeleton on the woman body.

In this section we are concerned with the formulation of the graph construction for triangular meshes and manifolds demonstrating that it is the quotient space of the input surface S with respect to an equivalence relation $\sim$. The proposed construction of G as $S/\sim$ enables to:

- verify that G depends only on the topology of S and on a finite set of representative points $\{p_1, \ldots, p_n\}$ in S of high-curvature values,
- verify that G is affine-invariant; this characteristic represents one of the main properties of G and of this theory not shared by other approaches,
- extract the information on G (e.g. compactness, connectivity, etc.) starting from S and exploiting the properties of the quotient space.

4.1. *Graph definition for triangle meshes*

Selected a point p_i in S we introduce the function

$$\begin{aligned} f_{p_i} : S &\longrightarrow \mathbf{N} \\ x &\mapsto f_{p_i}(x) := \min\{k : x \in T(N^k(i))\} \end{aligned}$$

, i.e., $f_{p_i}(x)$ is the minimal *topological distance* between p_i and x.

We can extend in a simple way the previous function to a finite set of vertices $\{p_1, \ldots, p_n\}$ as

$$\begin{aligned} f : S &\longrightarrow \mathbf{N} \\ x &\mapsto f(x) := \min_{k=1,\ldots,n}\{f_{p_k}(x)\} \end{aligned}$$

, i.e., f assigns to x its minimal topological distance with respect to the case of more than one vertex ($n = 1, f = f_{n_1}$).

Starting from f and S we are able to construct the relation $\sim$ as follows:

$$p, q \in S, \;\; p \sim q \;\text{ iff }\; f^{-1}(f(p)) \cap f^{-1}(f(q)) \neq \emptyset. \tag{4}$$

First of all, (4) implies that if $f(p) \neq f(q)$ then $p \not\sim q$; in fact, we have

$$f^{-1}(f(p)) \cap f^{-1}(f(q)) = f^{-1}(f(p) \cap f(q)) = f^{-1}(\emptyset) = \emptyset.$$

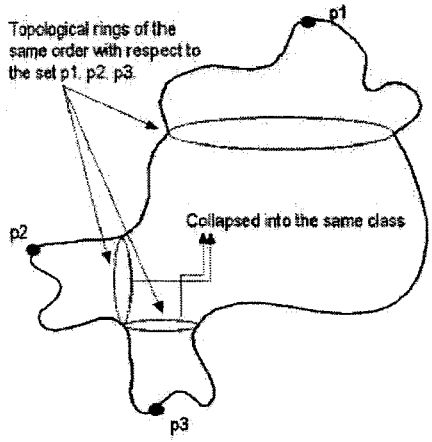

Fig. 13. Example of topological rings on a manifold.

In other words, necessary condition for $p \sim q$ is that $f(p) = f(q)$, that is, p and q have the same topological distance from the selected set of vertices $\{p_1, \ldots, p_n\}$. Secondly, two points p and q are in relation with respect to $\sim$ if and only if they have non-disjoint topological rings (i.e. $f^{-1}(f(p)) \cap f^{-1}(f(q)) \neq \emptyset$) of the same order (i.e. $f(p) = f(q)$).

From the previous relations it follows that

$$G = S/\sim = \{[x] : x \in S\}$$

where the class of x is represented by the set

$$[x] := \{y \in S : y \sim x\}.$$

Furthermore, the following conditions hold:

- $[x] \neq \emptyset, \forall x \in S$ (i.e. every class is not empty),
- $x \sim y \Rightarrow [x] \cap [y] = \emptyset$ (i.e. two vertices which satisfy the relation $\sim$ have non-empty intersection. Generally, the inverse condition is not true because $\sim$ is not transitive),
- $\bigcup_{x \in S}[x] = S$ (i.e. $\{[x]\}_{x \in S}$ represents a cover of S).

4.2. *Graph definition for manifolds*

We want to extend the previous model to a compact manifold without boundary embedded in $\mathbf{R}^3$ with the Euclidean topology underlining the general application of our model for the extraction of an affine-invariant shape description. In the following we review definitions and concepts on topology introducing the basic notions and referring to [5] for further readings. The structure of the section reflects that of the previous one facilitating the parallelism between the continuous case study and the discrete one which has been used for the implementation of the algorithm.

Introduced a topological space (X, τ), we define as

- *induced topology of X in $S \subseteq X$*: the topology τ_S defined as

$$\tau_S := \{A \cap S : A \in \tau\},$$

- *local base of p in X*: the family B_p consisting of neighborhoods of the point p such that for every neighborhood U of p there is a set $V \in B_p$ such that $V \subseteq U$,

- *boundary of $A \subseteq X$*: $\partial A := \overline{A} \cap \overline{X - A}$, that is, the intersection between the closure of the set A and its complement $(X - A)$ in X.

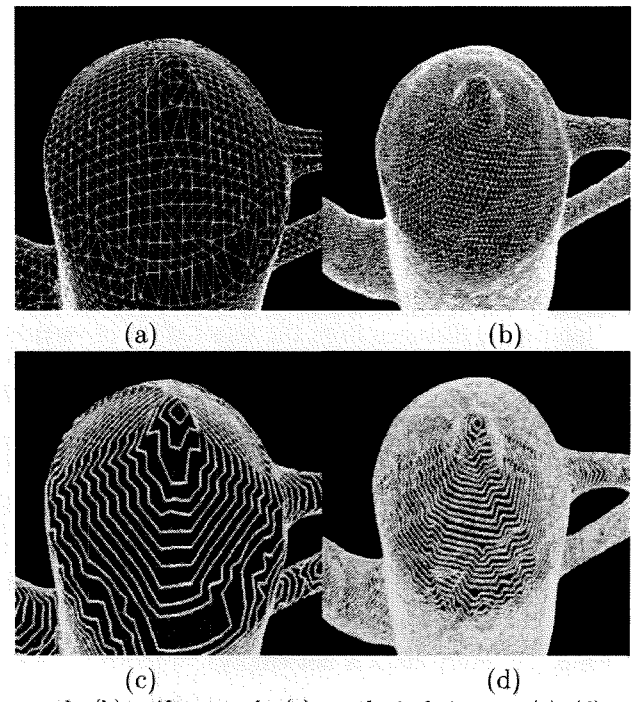

Fig. 14. (a) Input mesh, (b) uniform mesh, (c) topological rings on (a), (d) topological ring on (b).

Given a point $p \in S$ we define, for every $R > 0$, the open ball of center p and radius R as

$$B(p, R) := \{x \in \mathbf{R^3} : \|\mathbf{x} - \mathbf{p}\|_2 < \mathbf{R}\}$$

and with $U(p, R)$ the connected component of p in $S \cap B(p, R)$. Indeed, we can associate to each point $p \in S$ the family of neighborhoods $\{U(p, R)\}_{R>0}$, with $U(p, 0) := \{p\}$, centered in p. From the previous relations we can derive the following properties which will be used for constructing the graph of S:

- $\{U(p, R)\}_{R>0}$ is a local base of the space S at the point p with respect to the topology τ_S induced by the Euclidean topology τ in S. This property follows using the definition of τ_S and the fact that the set $\{B(p, R)\}_{R>0}$ is a local base of p in $(\mathbf{R^3}, \tau)$.

- $R_1 < R_2 \Rightarrow U(p, R_1) \subseteq U(p, R_2)$: in fact, $R_1 < R_2 \Rightarrow B(p, R_1) \subseteq B(p, R_2) \Rightarrow S \cap B(p, R_1) \subseteq S \cap B(p, R_2) \Rightarrow$ the connected component of p in $S \cap B(p, R_1)$ is a subset of that in $S \cap B(p, R_2)$.

Introduced the counterparts of the concepts defined for the triangular mesh, we can extend the previous functions as described in the following. Chosen a point $p \in S$, we define the map

$$\begin{aligned} f_p : \mathbf{R^3} &\longrightarrow \mathbf{R} \\ x &\mapsto f_p(x) := \|p - x\|_2 \end{aligned}$$

and then, fixed a set of points $P := \{p_1, \ldots, p_n\} \subseteq S$, we construct its extension to the set P as

$$\begin{aligned} f : S &\longrightarrow \mathbf{R} \\ x &\mapsto f(x) := \min_{k=1,\ldots,n}\{f_{p_k}(x)\}. \end{aligned}$$

The function f is continuous because it is the composition of the continuous maps

$$\begin{aligned} (f_{p_1}, \ldots, f_{p_n}) : S &\longrightarrow \mathbf{R^n} \\ x &\mapsto (f_{p_1}(x), \ldots, f_{p_n}(x)) \end{aligned}$$

and

$$\begin{aligned} \min : \mathbf{R^n} &\longrightarrow \mathbf{R} \\ (x_1, \ldots, x_n) &\mapsto \min_{i=1,\ldots,n}\{x_i\}. \end{aligned}$$

Indeed, in analogy with the previous section, we can introduce the relation $\sim$ as: $p, q \in S$ $p \sim q$ if and only if we can choose $R > 0$ such that $f(p) = f(q)$ and p, q belong to the same connected component of $f^{-1}(f(p))$. In other words, necessary and sufficient condition for $p \sim q$ is that p and q have the same topological distance from the selected set of points $\{p_1, \ldots, p_n\}$ and they belong to the connected component of the pre-image of their (common) value $f(p)$. The relation $\sim$ is symmetric, reflexive and transitive because it is the intersection of two equivalence relations (i.e. function equality and membership to the same connected component). Using the properties of the quotient space, we deduce that $\sim$ induces in S a decomposition into a family of non-empty, disjoint topological classes.

If the input surface S is compact/connected then G is compact/connected; anyway, the canonical projection

$$\begin{aligned} \pi : S &\longrightarrow G = S/\sim \\ x &\mapsto [x] \end{aligned}$$

is continuous with respect to the quotient space topology (i.e. $A \subseteq G$ is open if $\pi^{-1}(A)$ is open in (S, τ)). Figure 15 shows the skeleton of the tea-pot with respect to different meshes of the input data set. Now we want to investigate the properties of $\sim$:

- reflexive: $\forall p \in S, p \sim p$,
- symmetric: $\forall p, q \in S, p \sim q \Rightarrow q \sim p$,
- transitive: $\forall p, q, r \in S, p \sim q, q \sim r \not\Rightarrow p \sim r$. In fact, the intersection of sets is not transitive on $P(X) := \{X : X \subseteq S\}$.

Remark 1 *The previous construction can be reduced to define the function f such that $Im(f) := \{f(x) : x \in S\} \subseteq \mathbf{N}$ choosing, for a given point $p \in S$, its local base as $B_p = \{S \cap B(p, kn)\}_{n \in \mathbf{N}}$, with $k \in \mathbf{R}^+$ step, and defining for every $x \in S$ $f(x) := \min_{k=1,\ldots,n}\{f_{p_k}(x)\}$ where $f_{p_i}(x) := \min\{n : x \in B(p_i, kn)\}$.*

Remark 2 *Even thought f is not a Morse function we can define a point $p \in M$ as* critical *if the topology of the surface changes in one of its neighborhoods, that is, if there exists a value $\epsilon > 0$ such that*

$$C_M(f(p) + \epsilon) \neq C_M(f(p)), \qquad or \qquad C_M(f(p) - \epsilon) \neq C_M(f(p))$$

where $C_M(\alpha)$ is the number of connected components of $f^{-1}(\alpha)$, $\alpha \in \mathbf{R}$. We underline that p is a critical point if and only if q is a critical point for all $q \in [p]$; this means that the previous definition introduces a class of critical points given by the iso-curve $[p]$ which locates a topological transition given by a different number of rings during the expansion on the input mesh. Starting from the definition of critical points we can define the topological segmentation *of M. If p is a critical point we introduce the following relation*

$$p\mathcal{R}q \iff \forall \epsilon \in [f(q), f(p)], C_M(\epsilon) = C_M(f(p))$$

and the segmentation is given by $M/\mathcal{R}$.

5. Properties and comparison

We want to present the main properties and distinctions of the graph G with respect to other approaches as the Reeb graph. This comparison is evaluated considering the topological properties of both graphs, as quotient spaces, and a set of experimental results which underline the main drawbacks of the previous theory for shape abstraction.

The complexity of the proposed graph, in terms of number of nodes and branches, depends on the shape of the input object and of the number of points $\{p_i\}_{i=1}^n$ which we have selected using the curvature estimation criterion. The construction of G is guided, in the first step, by the topology of the mesh through the connectivity relations in F and, secondly, by the geometry V which influences the chosen representative point p for its equivalence class $[p]$. The only requirement for an optimal construction of the graph deals with a uniform mesh finalized at having a topological distance between points to which corresponds a medium step on the mesh (see Figure 14 and 15).

The graph structure is not incremental in the sense that if we add a point p_{n+1} to the set $\{p_1, \ldots, p_n\}$, which is used for the construction of G, the new graph $\tilde{G}$ defined by $\{p_1, \ldots, p_n, p_{n+1}\}$ is not achieved adding to G the new branch starting from p_{n+1}.

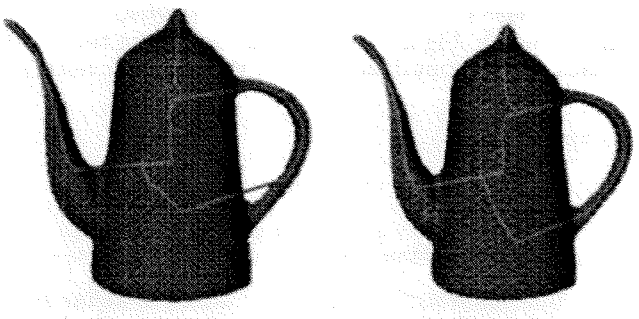

(a) (b)

Fig. 15. (a) Skeleton on the original data set, (c) skeleton on the refined mesh.

Our graph is affine-invariant (translation, rotation, scaling) because the function f which has been used for defining the relation $\sim$ and the quotient space G does not rely on a local system of coordinates in which the object surface is embedded as it happens in the case of the Reeb graph constructed, for example, using the height function (see Figure 16). However, we want to stress that both graphs are built in the same way choosing only two different functions. More precisely, our graph (the Reeb graph) codes the surface shape by analyzing the evolution of topological arcs (contours) obtained by the mesh topology (intersecting the surface with a family of planes along a chosen direction). On the other hand, if the curvature evaluation process does not recognize at leat one feature region (e.g. surfaces with constant curvature values such as spheres and torii), our approach is not useful to extract a description of the shape; on the contrary, the height function always guarantees to get a result. Other examples are given in Figure 17.

An interesting question is: does a relation between them exist? In other words, which hypothesis on S ensures that the related quotient spaces are homeomorphic?

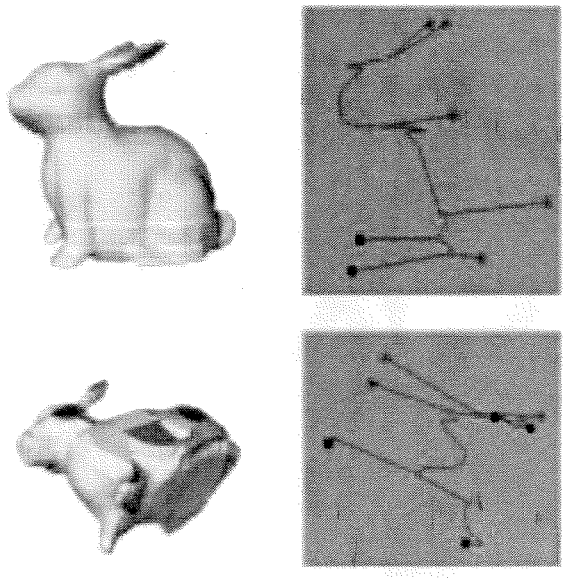

Fig. 16. Reeb Graph on the rabbit with respect to different functions.

6. Conclusions and future works

The starting point of this work is represented by previous approaches on shape abstraction attempting to propose possible extensions of the Reeb graph which represents the core of our model.

The graph described in this paper represents the first step toward the construction of a complete framework for shape abstraction, analysis and comparison. One of the most involving application that we foresee and we want to approach is shape matching. The affine-invariant structure of this graph and its description as quotient space enable to convert the matching problem between two graphs G and H into a multiple framework whose solution is achieved defining a matching function which is an homeomorphism between G and H plus a penalty function which takes into account the geometry of the related objects.

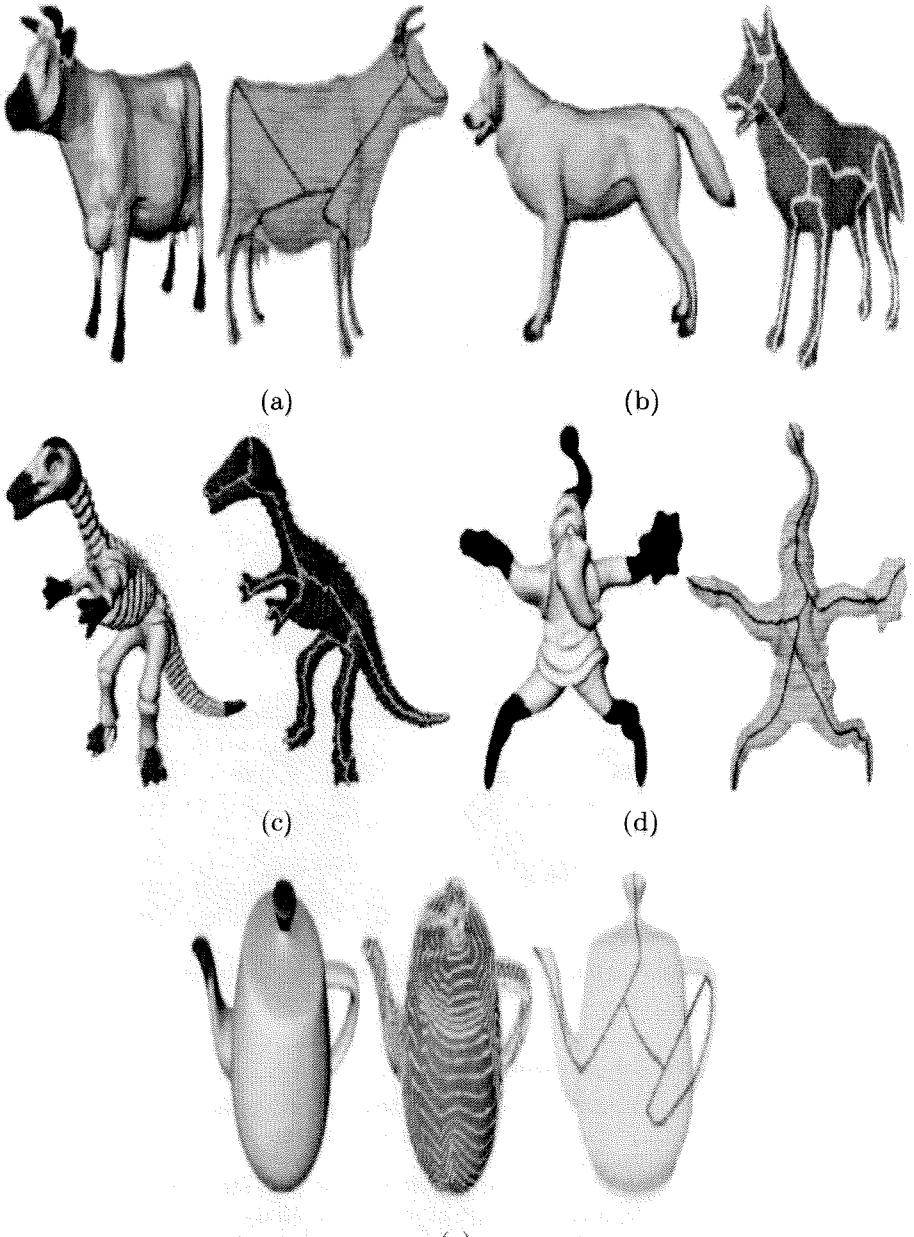

Fig. 17. Example of skeletons on different objects.

Acknowledgement

Special thanks are given to the Computer Graphics Group of IMATI-GE/CNR, and in particular to B. Falcidieno and M. Spagnuolo. This work has been supported by the Bilateral Project between GVU/Gatech (USA) and IMATI-GE/CNR "Surface Analysis" (URL: http://www.ima.ge.cnr.it/ima/personal/CGG/SurfaceAnalysis.html).

References

1. M. Attene, S. Biasotti, M. Spagnuolo, "Re-meshing Techniques for Topological Analysis", in *Proceeding of Shape Modeling International 2001*, IEEE Press, Genoa, May 2001, 142-151.
2. S. Biasotti, B. Falcidieno, M. Spagnuolo, "Extended Reeb Graphs for Surface Understanding and Description", in *Proceedings of the* 9^{th} *Discrete Geometry for Computer Imagery Conference, LNCS*, Springer Verlag, Uppsala, 2000.
3. H. A. Blum, "Transformation for Extracting New Descriptors of Shape", *Models for Perception of Speech and Visual Form*, MIT Press 1967, 362-381.
4. M. Desbrun, M. Meyer, P. Schroeder, A.H. Barr, "Discrete Differential Operators for Triangulated 2-manifolds", in *VisMath 2002, Proceeedings*, "Visualization and Mathematics III", Springer Verlag, Berlin, 22-25 May 2002.
5. R. Engelking, K. Sielucki, *Topology: a geometric approach*, Sigma Series in Pure Mathematics, Volume 4, Heldermann Verlag, Berlin, 1992.
6. B. Falcidieno, M. Spagnuolo, "Geometric Reasoning for the Extraction of Surface Shape Properties", *Communicating with the Virtual World*, N.Magnenat Thalmann and D. Thalmann (Eds.), Springer-Verlag, (1993)
7. B. Falcidieno, M. Mortara, G. Patanè, J. Rossignac, M. Spagnuolo. *Tailor: understanding 3D shapes using curvature*, Rapporto Tecnico N. 9/2001, Istituto per la Matematica Applicata, Consiglio Nazionale delle Ricerche.
8. R.C. Gonzales, R.E.Woods, *Digital Image Processing*. Reading, MASS.: Addison-Weshley, 1992.
9. V. Guillemin, A. Pollack, *Differential Topology*, Englewood Cliffs, NJ: Prentice-Hall, 1974.
10. B. Hamman, "Curvature Approximation for Triangulated Surfaces", *Computing Suppl.* 8, 1993, 139-153.
11. M. Hilaga, Y. Shinagawa, T. Kohmura, T.L. Kunii, "Topology Matching for Fully Automatic Similarity Estimation of 3D Shapes", in *Computer&Graphics, Proceeding of Siggraph 2001*, Los Angeles, 2001.
12. F. Lazarus, A. Verroust, "Level Sets Diagrams of Polyhedral Objects", in *ACM Solid Modeling '99*, Ann Arbour, Michigan, USA, 1999.
13. F. Lazarus, A. Verroust, "Extracting skeletal curves from 3D scattered data", in *The Visual Computer*, vol. 16, N. 1, 15-25, 2000.
14. M.M. Lipschutz, *Theory and Problems of Differential Geometry*. Schaum's Outline Series.
15. J. Milnor, *Morse Theory*, Princeton University Press, New Jersey, 1963.
16. M. Mortara, M. Spagnolo, *Hierarchical Representation of 2D Polygons based on Approximate Skeletons*, Technical Report N. 8/2000, Istituto per la Matematica Applicata, Consiglio Nazionale delle Ricerche.
17. M. Mortara, G. Patanè, "Affine-invariant skeleton of 3D-shapes", in *IEEE Proceedings of International Conference on Shape Modeling International and Applications 2002*,
18. M. Mortara, G. Patanè, M. Spagnuolo, B. Falcidieno, J. Rossignac, "Blowing Bubbles

for the Multi-scale Analysis and Decomposition of Triangle Meshes". To appear in *Algorithmica*, Special Issues on Shape Algorithms.
19. K. Polthier, M. Schmies, "Straighhtest Geodesic polhedral Surfaces". In H.C. Hege and K. Polthier, editors, *Mathematical Visualization*. Springer Verlag, 1998.
20. G. Reeb, "Sur les points singuliers d'une forme de Pfaff completement integrable ou d'une fonction numerique", *Comptes Rendus Acad. Sciences*, Paris, 1946, 222: 847-849.
21. E. C. Sherbrooke, N. M. Patrikalakis, E. Brisson, "An Algorithm for the Medial Axis Transform of 3D Polyhedral Solids", *IEEE Transaction on Visualization and Computer Graphics*, Vol. 2, N.1, March 1996.
22. Y. Shinagawa, T.L. Kunii, Y.L. Kergosien, "Surface Coding Based on Morse Theory", *IEEE Computer Graphics & Applications*, 1991, pp. 66-78.
23. G. Taubin, "Estimating the Tensor Curvature of a Surface from a Polyhedral Approximation", in *Fifth International Conference on Computer Vision (ICCV'95)*.
24. E. Trucco, A. Verri, *Introductory to techniques for 3-D computer vision*. Prentice Hall, 1998.
25. G. Wyvill, C. Handley, "The 'Thermodynamics' of Shape", in *Proceedings of Shape Modeling International 2001*, IEEE Press, Genova, Italy, May 2001, 2-8.
26. Z. Wood, M. Desbrun, P. Schroeder, M. Breen, "Semi Regular Mesh Extraction From Volumes", in *Procedings of IEEE Visualization 2000*, October 2000, pp. 275-282.